A Study of General Three-Dimensional Boundary-Layer Problems by an Exact Numerical Method

JOE DER JR.*
Northrop Corporation, Hawthorne, Calif.

Complete solutions of the three-dimensional laminar boundary layer on a 15° half-angle blunted cone at angles of attack using Newtonian pressure distribution are presented. The method of calculation is a modification of the Raetz explicit finite-difference procedure. Results presented include inviscid and boundary-layer limiting streamlines, singular points of separation, and sample zones of dependence and influence. It has been found that the crossflow velocity derivative, which is neglected in the small crossflow theory, is actually large and dominates the three-dimensional boundary-layer separation process. Based on the influence principle, it is shown that solutions obtained by calculating along planes of symmetry is valid. Three-dimensional singular points of separation can be determined, but the complete region or an ordinary line of separation seems to require a more realistic specification of the pressure distribution than the Newtonian and/or the consideration of viscid-inviscid interaction.

Nomenclature

B_i = differential equation coefficients
c_p = coefficient of pressure
i,j,k = lattice indices in ξ, η, and ζ directions
l = total enthalpy
L = length
N = boundary-layer outer edge absolute viscosity
p = static pressure
Q = boundary-layer edge total velocity
R = Reynolds number $= \Lambda' Q' L_0' / N_0'$; also radial distance
$\mathfrak{R}$ = universal gas constant
s = velocity component parallel to local boundary-layer edge inviscid stream
ds = an element of length
t = temperature
u = longitudinal velocity (component in the ξ direction)
U = boundary-layer edge longitudinal velocity (component in the ξ direction)
v = transverse velocity (component in the η direction)
V = boundary-layer edge transverse velocity (component in the η direction)
w = normal velocity (component in the ζ direction)
x,y,z = curvilinear distance in the ξ, η, and ζ directions
α = angle of attack; also metric coefficient in the ξ direction
β = metric coefficient in the η dierection
γ = metric coefficient in the ζ direction
δ = boundary-layer thickness
Δ^* = three-dimensional boundary-layer displacement thickness
ϵ = real-gas compressibility factor
ξ,η,ζ = boundary-layer curvilinear coordinates
θ = meridian angle
ϕ = complement of freestream flow deflection angle
κ = thermal conductivity
Λ = boundary-layer edge inviscid density
λ = density
ν = absolute viscosity
σ = specific heat at constant pressure
φ = shear parameter defined by Eq. (3)

Subscripts and superscripts

$(\ )_0$ = reference quantity, usually referred to freestream conditions
$(\ )'$ = dimensional quantity
$(\ )_{wall}$ = condition at the wall

Presented as Paper 69-138 at the AIAA 7th Aerospace Sciences Meeting, New York, January 20-22, 1969; submitted February 11, 1969; revision received September 21, 1970. This work was supported by AFFDL, Air Force System Command, under Contract AF33(657)-8673. The author wishes to acknowledge the assistance given by H. L. Handy in the programing and analyses. Special thanks are given to W. A. Rockwell, J. L. Patterson, and A. B. Lewis of AFFDL, who contributed valuable time in obtaining the present results.

* Senior Technical Specialist, Research and Technology Section, Aircraft Division. Associate Fellow AIAA.

I. Introduction

THE importance of three-dimensional boundary layer in practical engineering problems has been recognized for many years. Because of the complexities of fully three-dimensional flows, most boundary-layer analyses have been devoted to two-dimensional or axially symmetric flows. Earlier treatments of three-dimensional boundary-layer problems were limited to approximate approaches. Because of the lack of exact and fully three-dimensional boundary-layer solutions, many important three-dimensional flow properties are still not fully understood. The purpose of the present study is to calculate some complete exact three-dimensional boundary-layer solutions for a typical body of revolution so that some important three-dimensional effects can be analyzed.

A general explicit finite-difference method of integrating the complete compressible three-dimensional laminar boundary-layer equations was first developed by Raetz.[1] It was used to determine the flow properties on a swept tapered wing with suction.[2] The method has been also applied to an ellipsoid at zero angle of attack under ideal and real gas flow conditions and to generalized three-dimensional bodies with spherical noses at angles of attack.[3] Other exact and fully three-dimensional boundary-layer methods have been developed recently by Cooke and Hall,[4,5] Dwyer,[6] and Wang.[7] In general, these methods utilize implicit schemes and have been tested on simple bodies in incompressible flows. Dwyer, for example, applied his method to determine flow properties over a flat plate assuming an incompressible potential flow around a semi-infinite cylinder oriented perpendicular to the plate.

Some recent reviews on three-dimensional laminar boundary layers were given by Mager,[8] Stewartson,[9] and Sherman.[10] Earlier exact solutions, but for specialized cases, were completed by Yohner and Hansen,[11] Moore,[12] and Reshotko.[13,14]

A series of similar incompressible three-dimensional boundary-layer solutions was calculated by Yohner and Hansen. Moore obtained special solutions along windward generator of a pointed cone and found that, in his case, where the pressure is constant along a generator, all boundary-layer quantities show parabolic similarity in meridian planes. Moore also found that, except for very small angles of attack, solutions are indeterminate or do not exist along the leeward generator beyond a certain angle of attack. Moore's solutions were later extended by Reshotko to include heat transfer and arbitrary Prandtl number.

Among the approximate methods of computation, the most popular approach has been the use of the small crossflow theory, which reduces the three-dimensional boundary-layer analysis to a quasi-two-dimensional boundary-layer calculation.[15-19] In essence, the small crossflow theory assumes that the velocity component and its derivatives normal to the external inviscid stream are negligible. This assumption uncouples the longitudinal and the transverse momentum equations. The longitudinal equation is reduced to the two-dimensional form, whereas the transverse equation becomes linear and can be solved independently. In application, the calculation follows a single inviscid streamline and is sometimes called the "streamline coordinate" system.

The small crossflow theory, in principle, has at least two drawbacks. One is that the quasi-two-dimensional calculation, in general, violates the Raetz's influence principle.[1,2] The influence principle states that, for each point on the body, there is a zone of dependence and zone of influence which take the shape of curvilinear wedges, with one opening in the upstream direction and the other in the downstream direction.[2] The two sides of the zones of influence and dependence are defined by the two streamlines of maximum and minimum angles passing through the normal to the body at the point in question. In general, the inviscid streamline is curved over the surface, and the centrifugal force is balanced by the crossflow pressure gradient. Since the pressure, according to the boundary-layer theory, is constant across the boundary layer, whereas the velocity varies, the curvature of the internal streamlines must vary to maintain the same centrifugal force. Thus, so long as the inviscid streamline at a given point on the body is curved, there exists upstream a zone of dependence and downstream a zone of influence, both of finite width.

Another drawback in the small crossflow theory is the neglected crossflow derivative term in the basic equations. Along a plane of symmetry, the crossflow velocity component is zero, and the wedges of influence and dependence collapse to an infinitesimal strip. The crossflow derivative, however, is generally finite and varies across the boundary layer. For bodies of revolution, its magnitude is usually large. It has been found from the present calculations that along planes of symmetry the term in the continuity equation containing the crossflow derivative is of the same order of magnitude as that for the longitudinal direction. With the crossflow derivative neglected, therefore, mass flow continuity requirement cannot be satisfied. Furthermore, it has been found, and also pointed out by Moore[12] and Dwyer,[6] that the crossflow derivative is a dominating term in determining three-dimensional boundary-layer separations.

The concept of the zone of influence along a plane of symmetry is somewhat different from the physical explanation given by Moore,[12] who described a zone of influence of finite width due to molecular diffusion. The dominating side or lateral effects in the neighborhood of the plane of symmetry actually come from the mass flow continuity requirement, and the information is contained in the term of the crossflow derivative for the plane of symmetry. In principle, within the boundary-layer approximation, and without consideration of molecular diffusion, the solution along a plane of symmetry (windward or leeward generator) is valid provided that the crossflow derivative terms are properly included. Because the crossflow velocity component is zero along the plane of symmetry, the crossflow derivative term disappears from the transverse momentum equation and is retained only in the continuity equation. Since Moore used a two-vector form of the boundary-layer equations, where the flow is described by two stream functions, the continuity equation was not explicitly expressed in the system. Thus, Moore found that it was necessary to differentiate the transverse momentum equations with respect to the transverse coordinate to maintain a meaningful system. The new equation is similar to the crossflow velocity equation but introduces additional terms that are functions of the crossflow velocity derivative, which is finite along planes of symmetry. In the usual form of the boundary-layer equations, however, the crossflow derivative within the boundary layer is not known. Raetz[1] suggested a technique that makes use of the limiting value of the nondimensional transverse velocity component, thus eliminating the internal transverse velocity derivative from the system. Details and sample results of calculation for planes of symmetry or general partial stagnation lines are presented.

The present method of computation is a modification of the procedure developed by Raetz.[1,2] The program used was developed for generalized three-dimensional body configuration.[3] The method has been extended to include the effects of real gases, and the central difference method of computing transverse derivatives has been replaced by a spline curve-fitting procedure. The spline technique, which is a piecewise cubit fitting procedure for an array of data points such that the first and second derivatives are continuous, allows either the first or second derivative to be specified along planes of symmetry. The spline technique also improves the numerical accuracy, with fewer lateral steps than a standard finite-difference technique. The computation is carried out in a body-fixed coordinate system, which is thus invariant with the angle of attack or flow condition. A unique feature of the method is that solutions can be obtained at, or near, singular points or lines such as a stagnation point, or line, the apex of a pointed body of revolution, etc. The starting solution, which is required for all boundary-layer calculations, can be located at the singular point or line and can be determined automatically by the present computational procedure utilizing an iterative technique. The iteration procedure, of course, is not necessary if a known starting solution is specified.

Complete ideal gas laminar boundary-layer solutions are presented for a 15° half-angle blunted cone at angles of attack. Solutions for cold and adiabatic wall conditions are compared. A three-dimensional method of characteristics procedure can be coupled with the present boundary-layer program for accurately determining the properties external to the boundary layer. For the present study, however, a Newtonian type of pressure distribution was used. An advantage of the Newtonian type of pressure distribution is that it is analytic, and thus the boundary data are smooth, a required condition for the calculation. From a prescribed pressure distribution, inviscid streamlines just external to the boundary layer are determined by satisfying the body surface irrotational flow condition.

II. Method

System of Equations

The steady boundary-layer equations in general three-dimensional, curvilinear, orthogonal coordinates ξ, η, and ζ are as follows:

ξ momentum

$$\frac{u'}{\alpha'}\frac{\partial u'}{\partial \xi} + \frac{v'}{\beta'}\frac{\partial u'}{\partial \eta} + \frac{w'}{\gamma'}\frac{\partial u'}{\partial \zeta} + \frac{u'v'}{\alpha'\beta'}\frac{\partial \alpha'}{\partial \eta} - \frac{v'^2}{\alpha'\beta'}\frac{\partial \beta'}{\partial \xi} = -\frac{1}{\lambda'\alpha'}\frac{\partial p'}{\partial \xi} + \frac{1}{\lambda'\gamma'}\frac{\partial}{\partial \zeta}\left(\frac{\nu'\partial u'}{\gamma'\partial \zeta}\right) \quad (1a)$$

η momentum

$$\frac{u'}{\alpha'}\frac{\partial v'}{\partial \xi} + \frac{v'}{\beta'}\frac{\partial v'}{\partial \eta} + \frac{w'}{\gamma'}\frac{\partial v'}{\partial \zeta} - \frac{u'^2}{\alpha'\beta'}\frac{\partial \alpha'}{\partial \eta} + \frac{u'v'}{\alpha'\beta'}\frac{\partial \beta'}{\partial \xi} = -\frac{1}{\lambda'\beta'}\frac{\partial p'}{\partial \eta} + \frac{1}{\lambda'\gamma'}\frac{\partial}{\partial \zeta}\left(\frac{\nu'}{\gamma'}\frac{\partial v'}{\partial \zeta}\right) \quad (1b)$$

Energy

$$\frac{u'}{\alpha'}\frac{\partial t'}{\partial \xi} + \frac{v'}{\beta'}\frac{\partial t'}{\partial \eta} + \frac{w'}{\gamma'}\frac{\partial t'}{\partial \zeta} = \frac{1}{\sigma'\lambda'}\left(\frac{u'}{\alpha'}\frac{\partial p'}{\partial \xi} + \frac{v'}{\beta'}\frac{\partial p'}{\partial \eta}\right) + \frac{\nu'}{\sigma'\lambda'\gamma'^2}\left[\left(\frac{\partial u'}{\partial \zeta}\right)^2 + \left(\frac{\partial v'}{\partial \zeta}\right)^2\right] + \frac{1}{\sigma'\lambda'\gamma'}\frac{\partial}{\partial \zeta}\left(\frac{\kappa'}{\gamma'}\frac{\partial t'}{\partial \zeta}\right) \quad (1c)$$

Continuity

$$\frac{\partial}{\partial \xi}(\beta'\gamma'\lambda'u') + \frac{\partial}{\partial \eta}(\alpha'\gamma'\lambda'v') + \frac{\partial}{\partial \zeta}(\alpha'\beta'\lambda'w') = 0 \quad (1d)$$

where ξ and η are the general downstream and lateral coordinates, respectively, defined along the body surface, ζ is the coordinate normal to the body surface, and α', β', and γ' are the metric coefficients or distance scale factors that are used to relate an element of arc length ds' as

$$ds'^2 = \alpha'^2 d\xi^2 + \beta'^2 d\eta'^2 + \gamma'^2 d\zeta^2$$

In general, the metric coefficients are functions of the ξ, η, and ζ coordinates. Within the boundary-layer approximation, however, where the thickness of the boundary layer is thin compared to its surface, α' and β', which describe the body surface geometry, can usually be assumed independent of the ζ coordinate.

Now ζ, as introduced by Raetz, is defined as a function of the longitudinal velocity component by

$$\zeta = [1 - (u'/U')]^{1/2} \quad (2)$$

where u' and U' are the dimensional internal and external (outer edge of the boundary layer) longitudinal velocity components, respectively; thus, the boundary layer is bounded between $\zeta = 0$ at the outer edge of the boundary layer, and $\zeta = 1$ at the body surface, where the velocity is zero. The square root is introduced to eliminate numerical singularity along the outer edge of the boundary layer and to obtain better numerical accuracy and more economical step sizes, since the normal velocity gradient in the boundary layer is generally large near the body surface and approaches zero at the outer edge of the boundary.

A shear parameter φ' is defined as

$$\varphi' = \frac{\nu'}{2\zeta}\frac{\partial}{\partial z'}\frac{u'}{U'} = -\frac{\nu'}{\gamma'} \quad (3)$$

The dimensional (primed) quantities used in the foregoing equations are nondimensionalized in the following manner:

$$x = \frac{x'}{L_0'} \qquad t = \frac{\Re' t'}{Q_0'^2}$$

$$\alpha = \frac{\alpha'}{L_0'} \qquad \nu = \frac{\nu'}{tN_0'}$$

$$u = \frac{u'}{Q'} \qquad \varphi = \frac{\nu'}{2\zeta}\frac{\partial}{\partial \zeta}\left(\frac{u}{U}\right) = -\frac{\nu}{\gamma}$$

$$y = \frac{y'}{L_0'} \qquad p = \frac{p'}{\Lambda_0' Q_0'^2}$$

$$\beta = \frac{\beta'}{L_0'} \qquad \kappa = \frac{\kappa'}{\Re' \nu'}$$

$$v = \frac{v'}{Q'} \qquad z = \frac{R^{1/2}}{\xi^* L_0'}\int_0 \frac{\lambda'}{\Lambda'}\,dz'$$

$$\gamma = \frac{\gamma'}{L_0'}\left(\frac{R^{1/2}}{\xi^*}\right)\left(\frac{\lambda'}{\Lambda'}\right) \qquad Q = \frac{Q'}{Q_0'}$$

$$w = \frac{w'}{U'}\left(\frac{\lambda'}{\Lambda'}\right)\xi^* R^{1/2} \qquad \sigma = \frac{\sigma'}{\Re'}$$

where subscript zero denotes reference quantities. Uppercase symbols denote boundary-layer external or outer edge quantities. Here, L_0' is an arbitrary reference length and R is a local Reynolds number defined as $U'\Lambda' L_0'/N'$. The quantity ξ^* was introduced by Raetz as a convenient positive constant or a function of ξ and η to remove singularities at stagnation points, lines, or leading edges where the inviscid velocity and/or the distance ξ becomes zero.

The equation of state,

$$p' = \epsilon'\lambda'\Re' t' \quad (4)$$

is introduced to eliminate the density λ', and the definition of ζ removes explicit dependence on u'. Furthermore, w' is eliminated by substituting its expression from Eq. (1a) into the remainder of Eq. (1), yielding the following system of equations for the three unknowns v, t, and φ:

$$B_1\frac{\partial v}{\partial \xi} + B_2\frac{\partial v}{\partial \eta} + (B_3 + B_5)\frac{\partial v}{\partial \zeta} = B_3\zeta\frac{\partial^2 v}{\partial \zeta^2} + B_6 \quad (5a)$$

$$B_1\frac{\partial t}{\partial \xi} + B_2\frac{\partial t}{\partial \eta} + (B_3 + B_5)\frac{\partial t}{\partial \zeta} = B_4\zeta\frac{\partial^2 t}{\partial \zeta^2} + B_7 + B_9\left(\frac{\partial v}{\partial \zeta}\right)^2 + B_{10}\left(\frac{\partial t}{\partial \zeta}\right)^2 + B_{11}\frac{\partial t}{\partial \zeta}\frac{\partial \varphi}{\partial \zeta} \quad (5b)$$

$$B_1\frac{\partial \varphi}{\partial \xi} + B_2\frac{\partial \varphi}{\partial \eta} + (B_5 - B_3)\frac{\partial \varphi}{\partial \zeta} = B_3\zeta\frac{\partial^2 \varphi}{\partial \zeta^2} + B_8 + B_{12}\frac{\partial v}{\partial \eta} + B_{13}\frac{\partial v}{\partial \zeta} + B_{14}\frac{\partial t}{\partial \xi} + B_{15}\frac{\partial t}{\partial \eta} + B_{16}\frac{\partial t}{\partial \zeta} - B_{17}\frac{\partial \varphi}{\partial \zeta}\frac{\partial t}{\partial \zeta} - B_{18}\zeta\frac{\partial^2 t}{\partial \zeta^2} + B_{19}\left(\frac{\partial t}{\partial \zeta}\right)^2 \quad (5c)$$

where $B_1 \ldots B_{19}$ are differential coefficients that are functions of boundary condition parameters,[3] the thermodynamic and transport properties of the fluid, and the nondimensional quantities v, t, and φ.[3]

Boundary Conditions

The boundary conditions required for the three-dimensional boundary-layer integration of general bodies of revolution are the inviscid flow (outer edge) boundary, wall boundary, side boundaries, and the initial or starting boundary as shown in Fig. 1.

The inviscid boundary data are the inviscid flow that may be obtained from numerical or experimental data. The properties required are the velocity vectors (magnitude and inviscid streamline direction), the pressure, and a temperature condition. In the calculations presented here, the pressure is obtained from the modified Newtonian formula

$$C_P = C_{P_{\max}}\cos^2\phi \qquad \phi < 45° \quad (6)$$

for a flow deflection angle higher than 45°, and from an empirical formula

$$C_P = C_{P_{\max}}/\{1 + \exp[4(\phi - \pi/4)]\} \qquad \phi \geq 45° \quad (7)$$

for a flow deflection angle of 45° or less, where the angle ϕ is a complement of the flow deflection angle and $C_{P_{\max}}$ is the pressure coefficient value at the stagnation point. The exponential curve is based on the matching of experimental data obtained for a sphere which improves the approximation at lower deflection angles, including the shadow region. From the known pressure distribution, the surface longitudinal and transverse components of the velocity, U' and V', are deter-

mined by assuming zero vorticity along the outer edge of the boundary layer and using the irrotational flow equation

$$\partial(\alpha' U')/\partial\eta = \partial(\beta' V')/\partial\xi \qquad (8)$$

The wall boundary data are the body geometry, boundary-layer suction or injection rates, and the thermal conditions. The body geometry is defined in terms of the metric coefficients α' and β' and their derivatives. The boundary-layer suction or injection is specified by the normal velocity component w at the wall. The wall thermal condition is either the wall temperature distribution or an arbitrary heat-transfer function. For the case of a specified wall temperature derivative, $(\partial t/\partial\zeta)_{\text{wall}}$ can be determined by Eq. (5b).

The side boundaries are planes of symmetry where

$$\partial t/\partial\eta = \partial\varphi/\partial\eta = 0 \qquad \partial^2 v/\partial\eta^2 = 0 \qquad (9)$$

The initial or starting profiles at boundaries, such as stagnation points, partial stagnation lines, or leading edges of a wing, are generally unknown. In the present method, the initial boundary-layer profiles can be either specified or calculated by the program. The starting solution, when unknown, can be first approximated and then determined by a successive substitution iteration technique using the same numerical procedure for the integration. The longitudinal derivatives, $\partial/\partial\xi$, of the three dependent variables, ν, t, φ are usually unknown, but they can be defined as zero by a proper choice of the coordinate ξ. For example, if ξ^2 is defined proportional to the surface distance x',

$$\partial/\partial\xi = \xi(\partial/\partial\xi^2) \propto \xi(\partial/\partial x')$$

which is zero for $\xi = 0$ at the start of the boundary layer, assuming that the derivatives with respect to x' are either zero or finite. In the iteration procedure, new values are calculated by

$$(\ )_{n+1} = (\ )_n + m[\partial(\ )/\partial\xi]\Delta\xi$$

where n denotes the cycle of iteration, m is an arbitrary fractional number needed to control numerical stability, and parentheses denote any quantity. The value $m = \frac{1}{2}$ has been suggested by Raetz[1] and has been found satisfactory for all cases calculated. Since the longitudinal derivatives are defined zero, the solution is converged when $\partial(\ )/\partial\xi \to 0$. The convergence of this method is slow but has the advantage that no special procedure is needed, and the computation, for most cases, can virtually be started automatically. The number of iteration cycles required by this technique varies from 50 to 1000, depending on the case and the approximation. The boundary layer over spherical nose section can be calculated by a simplified axisymmetric program for the blunted cone at an angle of attack. The starting solution, located at the stagnation point, is only two-dimensional. The starting solution for the cone, however, is located at the sphere-cone juncture, and can be obtained by interpolating and transforming the results computed for the sphere.[3]

Finite-Difference Procedure

The finite-difference integration procedure is a modification of the procedure described in Refs. 1 and 2. The integration is carried out by a "leap-frogging" technique similar to that described in Ref. 21, for a simple two-dimensional calculation. In the present method, the first derivatives of ξ and ζ in Eqs. (5a–5c) are replaced by ordinary central differences. The second derivative $\partial^2(\ )/\partial\zeta^2$ is approximated by

$$[\partial^2(\ )/\partial\zeta^2]_{i,j,k} \cong [(\ )_{i,j,k+1} - (\ )_{i+1,j,k} - (\ )_{i-1,j,k} + (\ )_{i,j,k-1}](\Delta\zeta)^2 \qquad (10)$$

which was obtained by replacing $(\ )_{i,j,k}$ with the approximation

$$(\ )_{i,j,k} \cong [(\ )_{i+1,j,k} + (\ )_{i-1,j,k}]/2 \qquad (11)$$

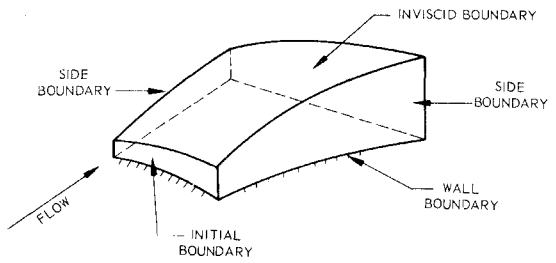

Fig. 1 Boundaries for three-dimensional boundary-layer integration.

The approximation of Eq. (11) was introduced to improve numerical stability.[21] In addition to the general requirement that both $\Delta\xi$ and $\Delta\zeta$ be small, it is required that $\Delta\xi \ll \Delta\zeta$. Typical values of $\Delta\xi$ and $\Delta\zeta$ are 0.0005 and 0.05, respectively. The transverse derivative $\partial(\ )/\partial\eta$ is calculated by a continuous first and second derivative technique, which is known as the "spline" fit.[3] This technique uniquely determines piecewise fitted cubic curves to a given array of data, such that the first and second derivatives are continuous. The technique also allows the end derivatives (either the first or the second) to be specified correctly.

Application

The calculation of a general three-dimensional boundary layer requires the definition of a body surface coordinate system, and the specification of the outer edge inviscid stream conditions, the wall thermal conditions, and the surface suction or injection rates.

The definitions of the coordinates ξ and η are arbitrary in direction and numerical variation but must follow certain general requirements. The coordinate ξ must increase in the general direction of the mainstream where the velocity component in the direction, u, must be positive. In addition, because of the Raetz's ζ transformation, which is a function of u, ξ should be oriented such that u, at any point (ξ,η) on the surface, decreases monotonically from the freestream value to zero at the wall.

Since the coordinate system in the present system of equations is orthogonal, the constant ξ and η lines must intersect perpendicularly. For a rotationally symmetric body, the definition of the coordinate system is trivial, since constant ξ and η can be the cross section and meridian planes, respectively. A numerical method of calculating orthogonal coordinate systems on general body configurations is given in Ref. 3. The numerical variation of ξ and η can be arbitrarily defined or transformed with respect to other physical variables. The arbitrary choices of ξ and/or η allow for control of numerical efficiency and mathematical singularities that might exist.

Special consideration must be given to regions where the inviscid stream velocity and/or the surface distance parameter ξ are zero. Under the present system, the usual singularities such as those along stagnation lines or points and sharp or blunt leading edges can be eliminated by defining ξ proportional to the square root of the surface distance along a reference η coordinate.

A criterion for a workable system is that the quantities or limiting quantities of the boundary conditions parameters[3] are either zero or finite. At singular regions such as stagnation points or leading edges, certain parameters may be indeterminate in form, and their limiting values must be determined using L'Hospital's rules.

Because the system being solved is strongly nonlinear, the input quantities must be consistent with boundary-layer equations and accurately specified so that a meaningful and numerically stable solution can be obtained. The inviscid velocity components (U',V'), the pressure (p'), and their

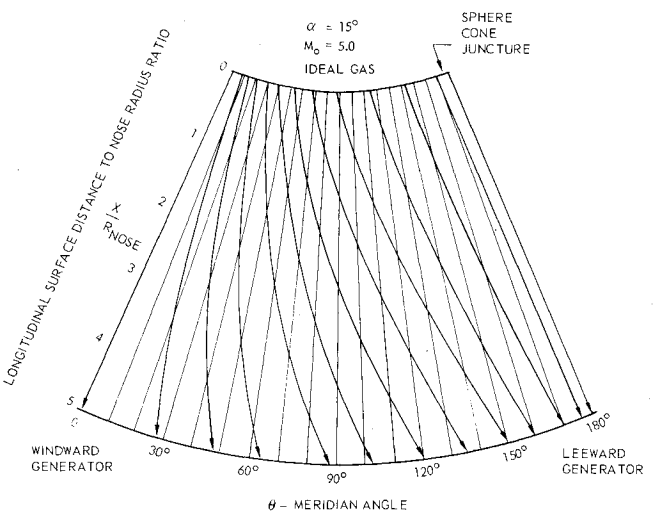

Fig. 2 Inviscid streamlines on a 15° half-angle blunted cone computed based on Newtonian/exponential pressure distribution ($\alpha = 15°$, $M_0 = 5.0$, ideal gas).

derivatives ($\partial V'/\partial\xi$, $\partial U'/\partial\eta$, $\partial p'/\partial\xi$) must satisfy the irrotational flow [Eq. (8)] or, if the flow is rotational, the complete vorticity equation.[1,2]

Along planes of symmetry, the crossflow velocity component is zero, but its derivative is finite. According to the influence principle, the zones of influence and dependence of any such point collapse to the planes of symmetry, and the analysis, therefore, is valid along a plane of symmetry without considering the complete boundary-layer surface. In the system described here, however, the side boundary condition, which involves only the transverse velocity derivative $\partial v/\partial\eta$, is unknown and cannot be determined unless solutions are obtained in the neighborhood of the plane of symmetry. This difficulty is overcome by a modification of the system given by Raetz[1] in which the nondimensional definition of v' is redefined as $v = v'/V'$ instead of $v = v'/Q$. Thus, although both v' and V' vanish, the limiting value of the ratio can still be finite. That is, in the new system

$$\lim_{v'\to 0} v = \frac{\partial v'/\partial\eta}{\partial V'/\partial\eta}$$

The term $\partial v'/\partial\eta$, therefore, can be eliminated from the system by expressing it as a function of the value at the boundary. Since all other η derivative terms are zero, the system is now independent of the η coordinate and becomes two-dimensional for the three dependent variables v, t, and φ. Thus, the equations for the new system are still the same [Eqs. (5a–5c)] but without η derivatives. The present system, although different in form, is equivalent to that obtained by differentiating the transverse momentum equation. One should note that the present limiting value v_i is actually proportional to the dimensional derivative $\partial v'/\partial\eta$.

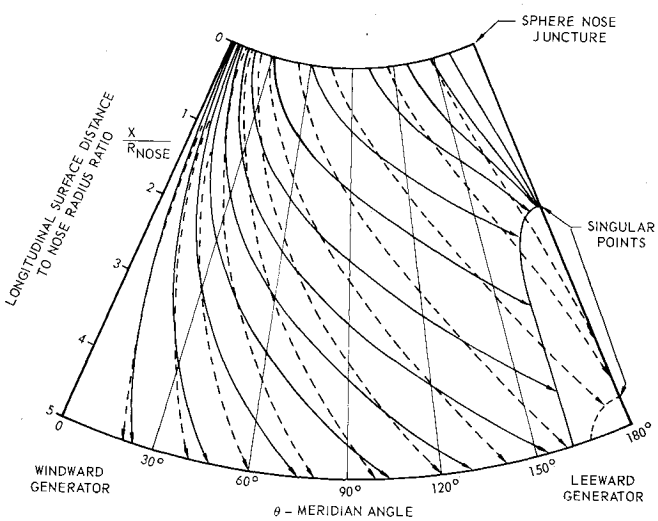

Fig. 3 Boundary-layer limiting streamlines on a 15° half-angle blunted cone [$\alpha = 15°$, $M_0 = 5.0$, ideal gas, —— adiabatic wall, – – – cold wall ($T_w = T_0$)].

III. Results

Complete three-dimensional laminar boundary layers for a 15° half-angle blunted cone at 5°, 10°, and 15° angles of attack have been calculated. The inviscid streamline pattern based on the Newtonian/exponential pressure distribution on the cone surface at 15° angle of attack is shown in Fig. 2. The maximum angle between an inviscid streamline and a meridian plane is of the order of 20°. Although the streamlines are calculated from an approximate pressure distribution, the pattern seems to be reasonable and will serve the purpose for the present study.

The corresponding boundary-layer limiting streamlines for cold and adiabatic wall conditions are plotted in Fig. 3. The wall temperature for the cold-wall case was assumed constant and equal to the freestream static temperature. The streamline patterns agree qualitatively with experimental data presented by Tracy[22] for a pointed cone. The maximum angles between the streamlines and the meridian planes here is of the order of 40° and 50° for cold and adiabatic wall conditions, respectively: a maximum stream angle difference across the boundary layer of approximately 20° to 30°. According to these calculations, the boundary layer separates at some point downstream along the leeward generator, with the adiabatic wall separation occurring somewhat earlier than the cold-wall separation. These wall temperature effects are consistent with two-dimensional flow where a heat transfer into the body tends to increase the skin friction and thus delay separation. The separation points here are the singular points of separation defined by Maskell.[20] Note that the boundary-layer limiting streamlines (initiating from the juncture at $\theta = 120°$ to 180°) converge toward, although not to, the singular point of separation. From the standpoint of mass flow continuity, the boundary layer must thicken rapidly along the leeward generator and finally separates from the

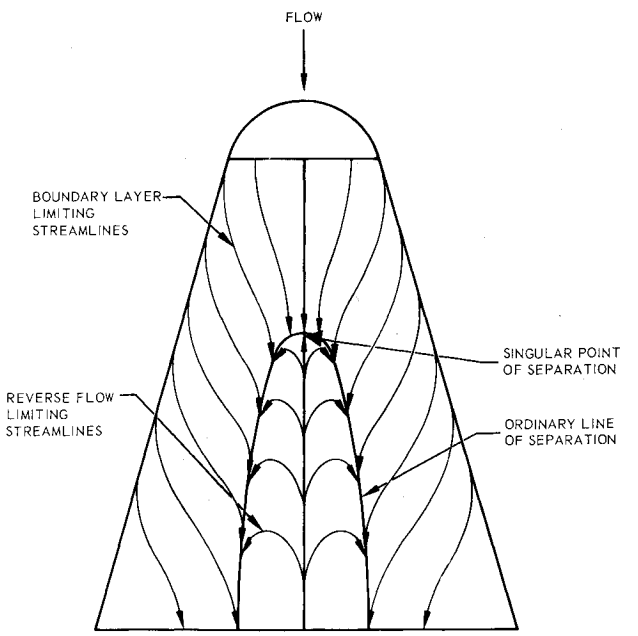

Fig. 4 Three-dimensional boundary-layer ordinary and singular points of separation.

surface as it approaches the singular point. In a two-dimensional boundary layer, the mass is always transported downstream. In three-dimensional boundary layer, the crossflows must "pile up" at the plane of symmetry. It is interesting to note that the inviscid streamline pattern depicted in Fig. 4 near and upstream of the singular point seems, at first glance, quite normal when compared with the more familiar two-dimensional or axially symmetric results. Mathematically, the effects that caused separation are coming from the crossflow velocity derivative or transverse pressure gradient, which does not exist in ordinary two-dimensional calculations. A similar observation has been pointed out by Dwyer.[6]

As mentioned earlier, Moore[12] found for pointed cones where the streamwise pressure gradient is zero along generators that all boundary-layer quantities show parabolic similarity in the meridian planes. He also found that the solution along the leeward generator is indeterminate or nonexistent beyond a certain small angle of attack. In the present calculation, the Newtonian type of pressure distribution also yields constant pressures along the leeward and windward generators. With a blunted nose, however, the solution on the nose up to the nose-body juncture is still two-dimensional. Thus, as long as the boundary layer remains attached along the nose, a starting three-dimensional boundary-layer solution will exist at the nose-body juncture. Since the boundary layer in the present case always tends to approach the asymptotic (or similar) type, based on Moore's analyses, one would expect that the solution will tend to become indeterminate at some point along the leeward generator. The distance for the boundary layer to separate, therefore, is the distance required for the flow to travel toward the asymptotic value. Thus, it may be concluded that the boundary layer on a blunted cone has less tendency to separate than that on a pointed cone.

In the present calculation, solutions can be obtained only for the portion of the boundary layer where the longitudinal shear component is positive. The criteria for three-dimensional boundary-layer separations were given by Maskell,[20] but a mathematical criterion has not yet been established. Three-dimensional boundary-layer separations, in general, are determined by the pattern of the boundary-layer limiting streamlines (streamlines that are close to the wall). An ordinary line of separation, as defined by Maskell, is the envelope of limiting streamlines running together as depicted in Fig. 4. Along a plane of zero transverse velocity component, the separation point is called the singular point of separation.

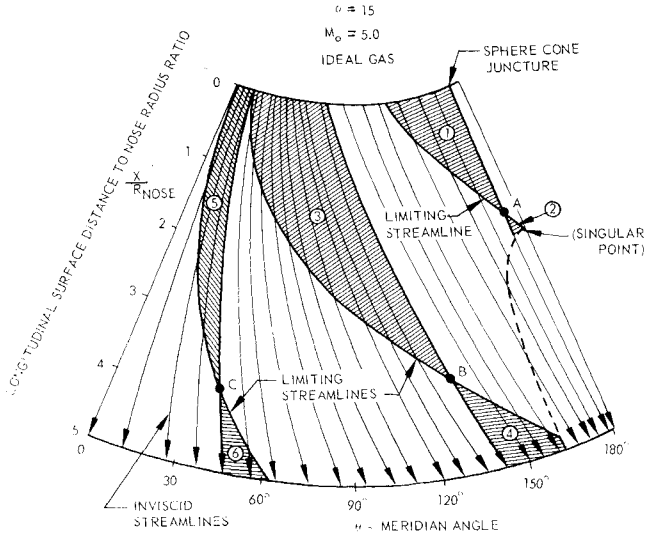

Fig. 5 Zones of dependence and influence of three points on a 15° half-angle blunted cone ($\alpha = 15°$, $M_0 = 5.0$, ideal gas).

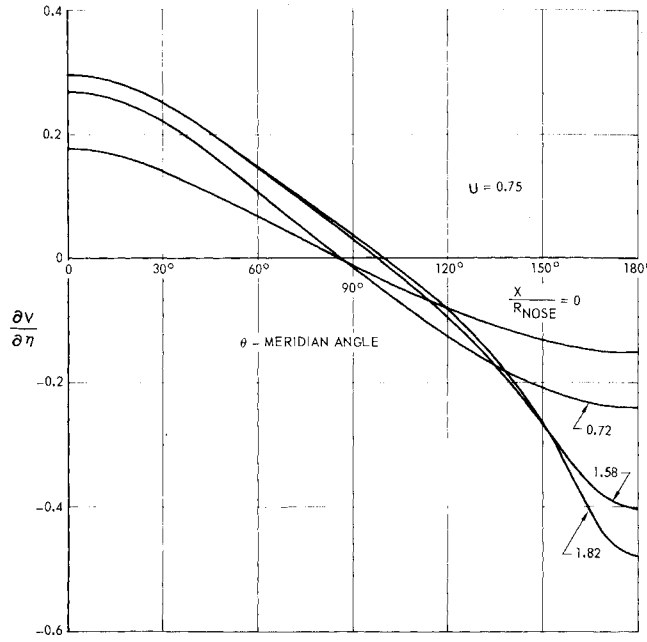

Fig. 6 Transverse variation of velocity derivative around a 15° half-angle blunted cone at 15° angle of attack.

Since the transverse velocity component is zero, the criterion for two-dimensional boundary-layer separations, zero wall shear, should also be applied at the singular point of separation.

The approximate separation line shown in Fig. 3 shows a region where solutions were not possible. The calculation, along a generator, was discontinued when the *longitudinal* component wall shear approached zero. The exact location of the point of zero wall shear generally required extrapolation from data upstream. The boundary-layer limiting streamlines calculated here do not indicate any pattern of an ordinary line of separation, even near a point of zero longitudinal wall shear. The reason for the failure in predicting the exact line of separation is probably due to the Newtonian pressure distribution, which has a minimum pressure along the leeward generator and thus has no adversed transverse pressure gradient. In realistic case, however, the problem is further complicated by the effects of viscid and inviscid interaction. Viscid-inviscid interaction as a result of boundary-layer separation, however, is beyond the scope of the present study.

Some samples of zones of dependence and influence of selected points on the cone surface for the adiabatic flow case are plotted in Fig. 5. The results cast some doubts on the validity of calculations that follow on a single inviscid streamline. Further study, however, is required to determine its order of effects.

The variations of crossflow velocity derivative with meridian angle for various body stations are plotted in Fig. 6. The maximum and minimum values for a given body station are always located along planes of symmetry for circular cross sections. Consequently, the crossflow effects should be also expected to be largest along planes of symmetry. A negative crossflow derivative along the leeward generator ($\theta = 180°$) indicates that the mass is flowing toward the generator. A direct comparison with the small crossflow theory is required to determine the flow derivative effects more exactly. It appears that the crossflow effects are much more pronounced in the leeward side, where the transverse velocity derivative is negative. In the calculation of Fannelop and Waldman,[23] for example, the small crossflow theory failed to predict an expected boundary-layer separation along the leeward side, even when a viscid-inviscid interaction was taken into consideration. On the other hand, the crossflow effects on the windward side do not seem to be as serious. Vaglio-

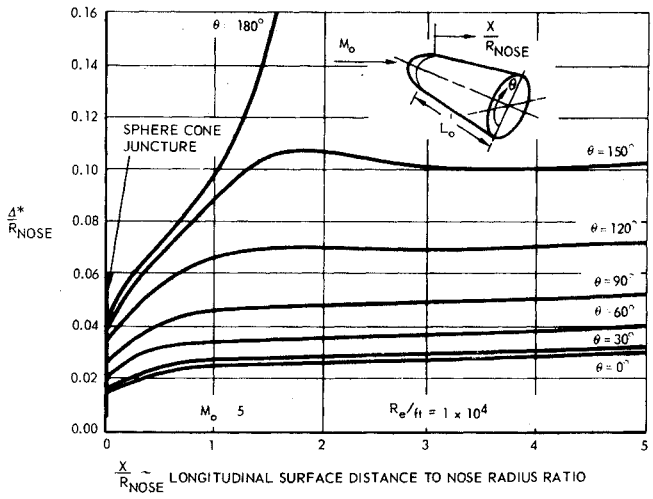

Fig. 7 Three-dimensional boundary-layer displacement thickness distribution on a 15° half-angle blunted cone at 15° angle of attack.

Laurin[24] found that, for cold wall condition, the small crossflow theory compared closely with Reshotko's exact calculation along the windward generator.[13,14]

The boundary-layer displacement thickness distributions are plotted in Figs. 7 and 8. Figure 7 shows the variation with respect to the longitudinal distance at constant meridian angle, whereas Fig. 8 shows an exaggerated polar plot for several cross sections. The displacement thickness along the windward side increases very slowly since the mass entrained by the boundary layer is pumped away by the low-pressure region in the leeward side.

Longitudinal and transverse velocity profiles (components parallel and perpendicular to meridian planes, respectively) for the adiabatic wall flow condition are plotted in Fig. 9 and 10 for longitudinal stations $X/R_{nose} = 0.72$ and 1.58. At $X/R_{nose} = 1.58$, which is a short distance ahead of the singular point of separation, the transverse velocity profiles (Fig. 10)

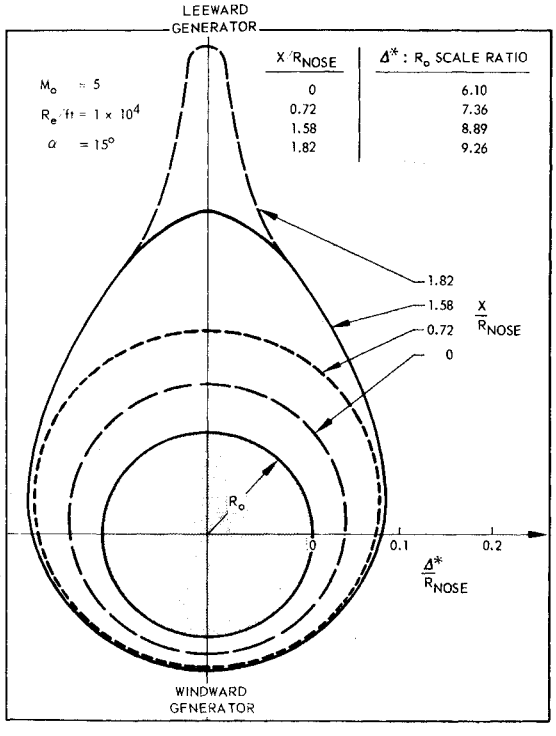

Fig. 8 Three-dimensional boundary-layer displacement thickness distribution around a 15° half-angle blunted cone at 15° angle of attack.

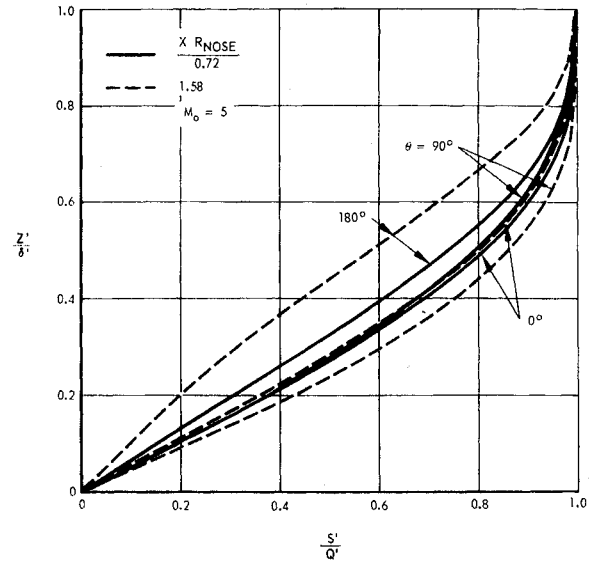

Fig. 9 Streamwise velocity profiles on a 15° half-angle blunted cone at 15° angle of attack.

show an overshoot within the boundary layer which is evidence of the large crossflow effects generated by the zone of dependence within the upstream boundary layers.

To study the relative magnitude of the crossflow derivative, the ratio of the transverse to the longitudinal mass flow derivatives in the continuity equation [Eq. (1d)] is plotted in Figs. 11 and 12. The ratio M_u/M_v is defined as

$$[(\partial/\partial\eta)(\alpha'\gamma'\lambda'v')]/[(\partial/\partial\xi)(\beta'\gamma'\lambda'u')]$$

Figure 11 shows the variation of the ratio with respect to the meridian angle for a constant $u = 0.75$ at various X/R_{nose} stations on the blunted cone at 10° angle of attack. The variation across the boundary layer is generally small and therefore is not presented. In general, the transverse mass flow derivative is of the same order as the longitudinal derivative, and the ratio has the maximum magnitude along planes of symmetry ($\theta = 0°, 180°$); Figure 12 shows comparisons of the ratio at 5°, 10°, and 15° angles of attack along the windward and leeward generators. The crossflow derivative term is still considerably large, even for a moderately small (5°) angle of attack.

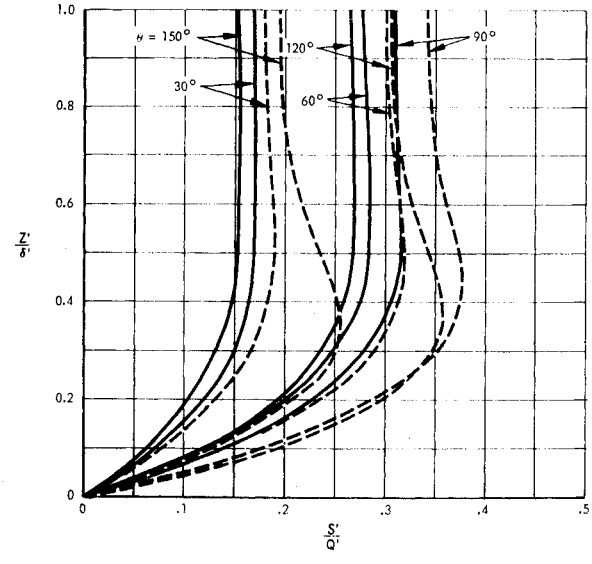

Fig. 10 Transverse velocity profiles on a 15° half-angle blunted cone at 15° angle of attack [——$(X/R_{nose}) = 0.72$, - - - $(X/R_{nose}) = 1.58$, $M_0 = 5.0$).

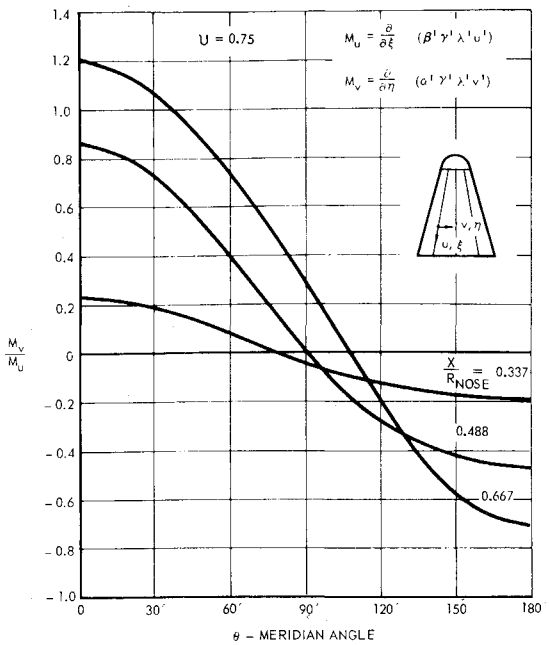

Fig. 11 Ratio of lateral to longitudinal velocity mass flow derivatives on a 15° half-angle blunted cone at 10° angle of attack.

To study the validity of the concept of calculating along planes of symmetry without the determination of the complete three-dimensional boundary layer, adiabatic wall partial stagnation line calculations along the windward and leeward generators were carried out for the same body and boundary conditions at 15° angle of attack. A comparison of the boundary-layer displacement thickness is shown in Fig. 13. The agreement is good for the windward generator but is only fair in the downstream portion of the leeward generator, where a rapid increase of the boundary-layer thickness exists. The differences may be because, in the complete three-dimensional boundary-layer calculation, the crossflow velocity derivative $\partial v/\partial n$ is computed numerically using the spline curve fit technique instead of the exact expression used in the partial stagnation line calculations. Thus, at a region where the boundary layer is rapidly growing, the numerical errors may increase. The exact cause, however, still remains to be explained.

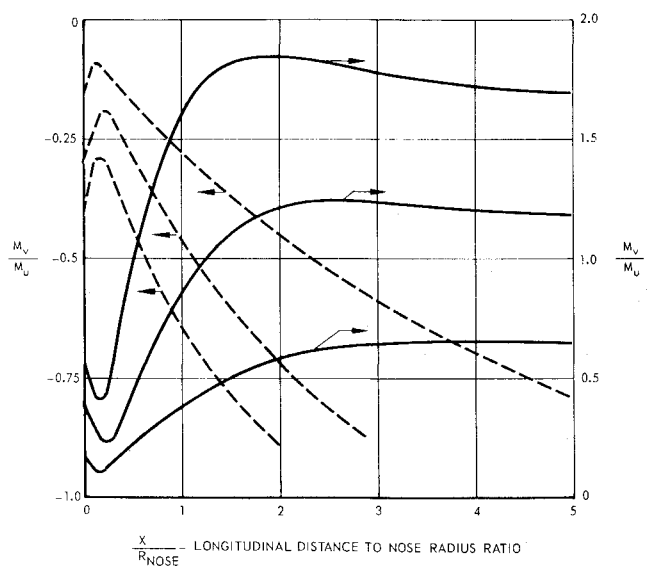

Fig. 12 Ratio of lateral to longitudinal mass flow derivatives of a 15° half-angle blunted cone at various degrees angle of attack (——windward generator, – – – leeward generator).

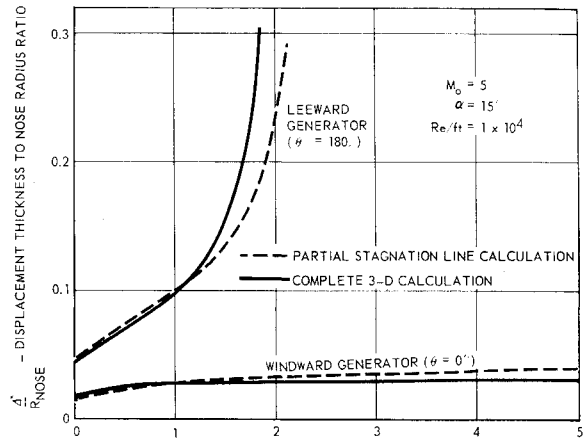

Fig. 13 Comparison of partial stagnation line calculation along planes of symmetry with a full three-dimensional boundary-layer calculation.

IV. Conclusions

Some properties of three-dimensional laminar boundary-layer flow have been analyzed using complete solutions obtained for a 15° half-angle blunted cone at angles of attack. It has been found that, for bodies of revolution, the crossflow velocity derivative, especially along planes of symmetry, is large and may not be neglected. The effects are more obvious along the leeward side, where the boundary layer tends to separate. On the other hand, the effects on the windward side do not seem to be as great, especially for cold-wall conditions. More studies, however, are still needed to determine the effects in detail. Based on Raetz's influence principle, the validity of a partial stagnation line calculation along the windward or leeward generator has been verified. It has been also found that singular points of separation can be determined, but the complete region of three-dimensional boundary-layer separation or ordinary lines of separation seem to require a more realistic specification of the pressure distribution than the Newtonian and/or the consideration of viscid-inviscid interaction.

Since only a Newtonian type of pressure distribution was used in the present study, the conclusions drawn can be classified as only qualitative. More quantitative studies should be conducted in the future to determine these effects more exactly.

References

[1] Raetz, G. S., "A Method of Calculating Three-Dimensional Laminar Boundary Layers of Steady Compressible Flow," NAI-58-73 (BLC-114), Dec. 1957, Northrop Corp., Hawthorne, Calif.

[2] Der, J., Jr. and Raetz, G. S., "Solution of General Three-Dimensional Laminar Boundary Layer Problems by an Exact Numerical Method," Paper 62-70, Jan. 1962, Inst. of the Aerospace Sciences.

[3] Powers, S. A., Niemann, A. F., Jr., and Der, J., Jr., "A Numerical Procedure for Determining the Combined Viscid-Inviscid Flow Fields over Generalized Three-Dimensional Bodies," AFFDL-TR-67-124, Vol. I, Dec. 1967, Air Force Flight Dynamics Lab., Wright-Patterson Air Force Base, Ohio.

[4] Cooke, J. C., "The Laminar Boundary Layer on an Inclined Cone," R & M 3530, Aug. 1965, Royal Aircraft Establishment.

[5] Hall, M. G., "A Numerical Method for Calculating Steady Three-Dimensional Laminar Boundary Layers," TR 67-145, June 1967, Royal Aircraft Establishment.

[6] Dwyer, H. A., "Solution of a Three-Dimensional Boundary Layer Flow with Separation," *AIAA Journal*, Vol. 6, No. 7, July 1968, pp. 1336–1342.

[7] Wang, K. C., "Three-Dimensional Laminar Boundary Layer Over Body of Revolution at Incidence, Part I, Method of Calcula-

tion," TR 68-14, Oct. 1968, Research Institute for Advanced Studies, Martin Marietta Corp.

[8] Mager, A., "Three-Dimensional Laminar Boundary Layers," *High-Speed Aerodynamics and Jet Propulsion: Theory of Laminar Flows*, edited by F. K. Moore, Vol. IV, Princeton University Press, Princeton, N.J., 1964, pp. 286–394.

[9] Stewartson, K., *The Theory of Laminar Boundary Layers in Compressible Fluids*, Oxford University Press, London, 1964, Chap. 5, pp. 99–121.

[10] Sherman, F. S., "Introduction to Three-Dimensional Boundary Layers," RM-4843-PR, April 1968, The Rand Corp., Santa Monica, Calif.

[11] Yohner, P. L. and Hansen, A. G., "Some Numerical Solutions of Similarity Equations for Three-Dimensional Laminar Incompressible Boundary Layer Flow," TN 4370, Sept. 1958, NACA.

[12] Moore, F. K., "Laminar Boundary Layer on Cone in Supersonic Flow at Large Angles of Attack," Rept. 1132, 1953, NACA.

[13] Reshotko, E. and Beckwith, I. E., "Compressible Laminar Boundary Layer Over a Yawed Infinite Cylinder with Heat Transfer and Arbitrary Prandtl Number," TN 3986, June 1957 NACA.

[14] Reshotko, E., "Laminar Boundary Layer with Heat Transfer on a Cone at Angle of Attack in a Supersonic Stream," TN 4152, Dec. 1957, NACA.

[15] Eichelbrenner, E. A. and Oudart, A., "Méthods de Calcul de la Couche Limite Tridimensionelle; Application a un Corps Fuselé Incliné sur le Vent," Publication 76, 1955, Office Nationale d'Etudes et de Recherches Aeronautiques.

[16] Cooke, J. C., "An Axially Symmetric Analogue for General Three-Dimensional Boundary Layers," R & M 3200, 1959, Aeronautical Research Council.

[17] Hall, M. G., "On the Momentum Integral Equations for Three-Dimensional Laminar Boundary Layers in Incompressible Flow," Rept. ACA-62, Nov. 1959, Australian Aeronautical Research Committee.

[18] Cooke, J. C., "Approximate Calculation of Three-Dimensional Boundary Layers," R & M 3201, Oct. 1959, Aeronautical Research Council.

[19] Fannelop, T. K., "A Method of Solving the Three-Dimensional Laminar Boundary Layer Equations with Application to a Lifting Re-Entry Body," *AIAA Journal*, Vol. 6, No. 6, June 1968, pp. 1075–1084.

[20] Maskel, E. C., "Flow Separation in Three-Dimensions," Rept. Aero 2565, 1955, Royal Aircraft Establishment.

[21] Dufort, E. C. and Frankel, S., "Stability Conditions in the Numerical Treatment of Parabolic Differential Equations," *Mathematical Tables and Other Aids to Computation*, Vol. VII, No. 43, July 1953, pp. 135–152.

[22] Tracy, R. R., "Hypersonic Flow Over a Yawed Circular Cone," Hypersonic Research Project Memo 69, 1963, California Institute of Technology.

[23] Fannelop, T. K. and Waldman, G. D., "Displacement Interaction and Flow Separation on Cones at Incidence to a Hypersonic Stream," *AGARD Conference Proceedings No. 30*, London, May 1968.

[24] Vaglio-Laurin, R., "Laminar Heat Transfer on Bunt-Nosed Bodies in Three-Dimensional Hypersonic Flow," WADC TN 58-147, 1958, Polytechnic Inst. of Brooklyn.

JULY 1971 AIAA JOURNAL VOL. 9, NO. 7

Methods for the Wind-Tunnel Measurement of Unsteady Nonlinear Aerodynamic Forces

MICHAEL JUDD*
Southampton University, England

Nonlinear aerodynamic forces are a feature of many shapes and flow regimes of current interest. Well-developed methods are available for the wind-tunnel measurement of unsteady aerodynamic loads using a linearized mathematical model. Free-flight and range techniques allow a more general representation. In this paper, nonlinear wind-tunnel methods are considered involving both random and deterministic excitation. It is suggested that a pure harmonic model motion (rather than excitation) has advantages both in analysis and in experimental accuracy. This has direct application to equipment in which the model is rigidly constrained to perform a pure motion. An analogue computer validation was performed. A quasi-steady variation and the extension to multidegree of freedom are discussed.

Nomenclature

a = parameter in the analogue, Eq. (22)
A_1,A_2,A_3,A_4 = amplitudes of frequency components in $E(t)$
a_{mn},a_m,b_m etc. = coefficients used in the expansion of the nonlinear aerodynamic moment M_A
B = structural damping coefficient
C,C_1,C_2 = integration constants
$e,e_0,E(t)$ = electrical analogue signals
e_{st} = coefficients defined by Eq. (15)
$f(\theta),g(\theta,\dot{\theta})$ = functions used in the description of the nonlinear moment M_A
I = model moment of inertia
$J_n(m\epsilon/\Omega)$ = Bessel function of the first kind with m and n integers
k = normalizing coefficient
K,K_1 = torsional and translational spring stiffnesses
l = characteristic model length
$M(t)$ = excitation moment
M_A = aerodynamic moment
M_b = model mass
$M_\theta,M_{\dot{\theta}},M_q$ etc. = aerodynamic stability derivatives
q_r = pitch rate
T = time delay
U_0 = undisturbed free stream velocity
w = translational velocity, $w = \dot{z}$
$W(\theta,\dot{\theta})$ = joint probability density function

Presented as Paper 70-573 at the AIAA 5th Aerodynamic Testing Conference, Tullahoma, Tenn., May 18–20, 1970; submitted June 16, 1970; revision received October 28, 1970. Work carried out at the Aerophysics Laboratory, Massachusetts Institute of Technology under NASA contract NAS 1-8658.

* Lecturer, Department of Aeronautics and Astronautics also Visiting Associate Professor, Massachusetts Institute of Technology during 1968–69.